

Supporting Information

Time-dependent dynamic multicolor afterglow of simple $\text{LiGa}_5\text{O}_8:\text{Eu}^{3+}/\text{Tb}^{3+}$ particles for advanced anticounterfeiting and encryption

Peng Zhang ^{a,b}, Wanying Xie ^b, Zhenbin Wang ^c, Zenggang Lin ^a, Xiuxiang Huang ^b,
Zhenghua Ju ^a, Weisheng Liu ^{a*}

^a Key Laboratory of Nonferrous Metal Chemistry and Resources Utilization of Gansu Province and State Key Laboratory of Applied Organic Chemistry, College of Chemistry and Chemical Engineering, Lanzhou University, Lanzhou 730000, P. R. China

^b College of Chemistry and Biology Engineering, Hechi University, Yizhou 546300, P. R. China

^c School of Chemistry and Chemical Engineering, Qinghai Normal University, Xining 810008, P. R. China

* Corresponding author:

Dr. Weisheng Liu, Email: liuws@lzu.edu.cn

Computational Methods

Spin-polarized calculations are performed using the Vienna Ab initio Simulation Package (VASP) and the project augmented wave potential. The functional of Perdew-Burke-Ernzerhof is used to calculate the exchange energy. The plane wave cutoff energy is set at 400 eV, the convergence criterion for the total energy is set at 10^{-5} eV, and the force acting on each atom is set at 0.02 eV/Å. Brillouin zone sampling is performed using the Gamma-center scheme with a k mesh of $3 \times 3 \times 3$. HSE06 functionals are used to calculate the band of the LiGa_5O_8 .

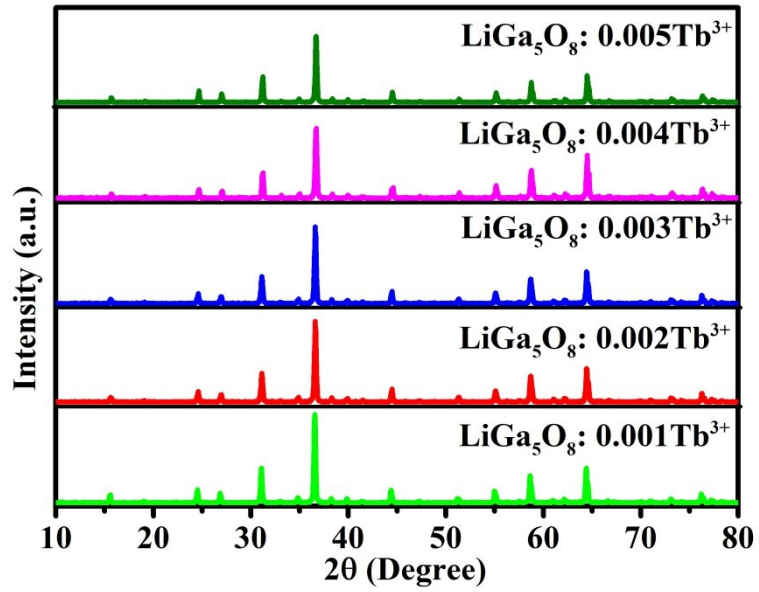


Fig. S1. XRD patterns of the $\text{LiGa}_5\text{O}_8:\text{Tb}^{3+}$ phosphors.

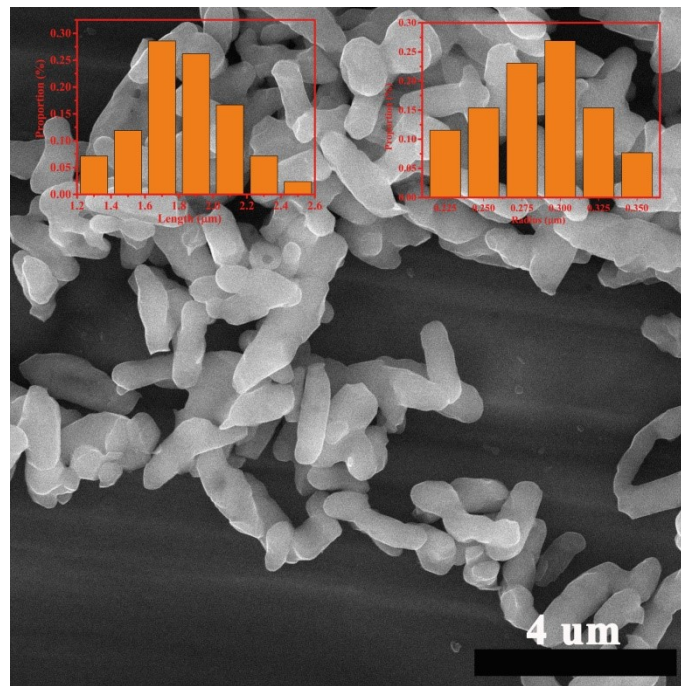


Fig. S2. SEM image of the $\text{LiGa}_5\text{O}_8:\text{Eu}^{3+}$ phosphors. The insets show the bar charts of the size distribution.

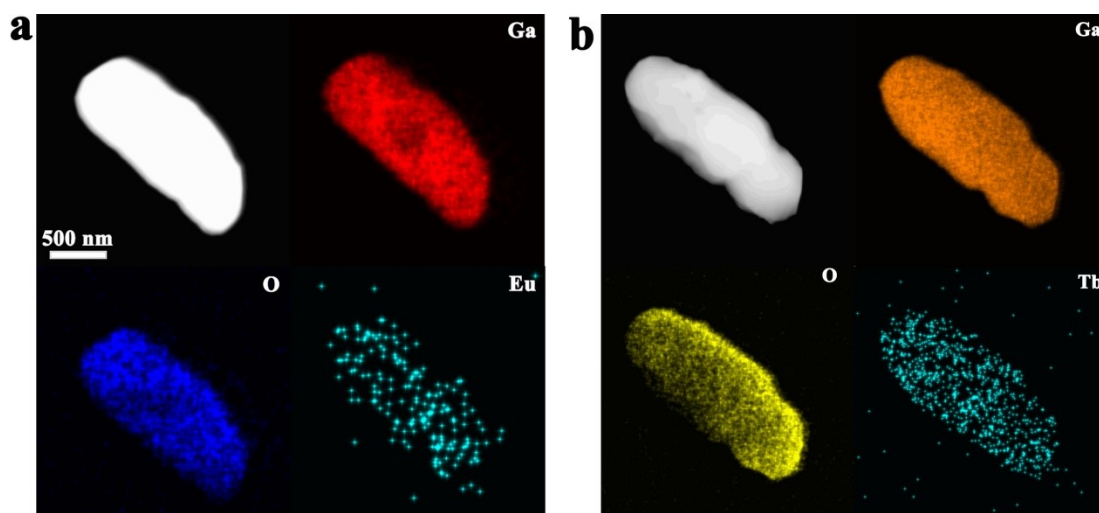


Fig. S3. Elemental distribution maps of the $\text{LiGa}_5\text{O}_8:0.003\text{Eu}^{3+}$ phosphors and the $\text{LiGa}_5\text{O}_8:0.003\text{Tb}^{3+}$ phosphors.

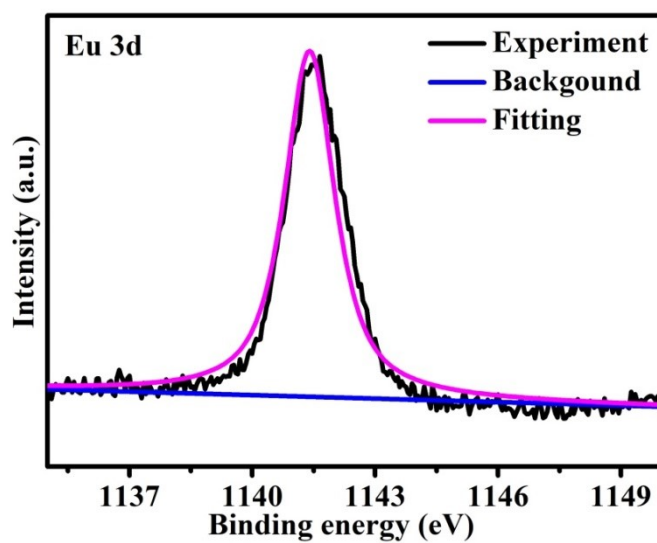


Fig. S4. High-resolution XPS spectra of Eu 3d.

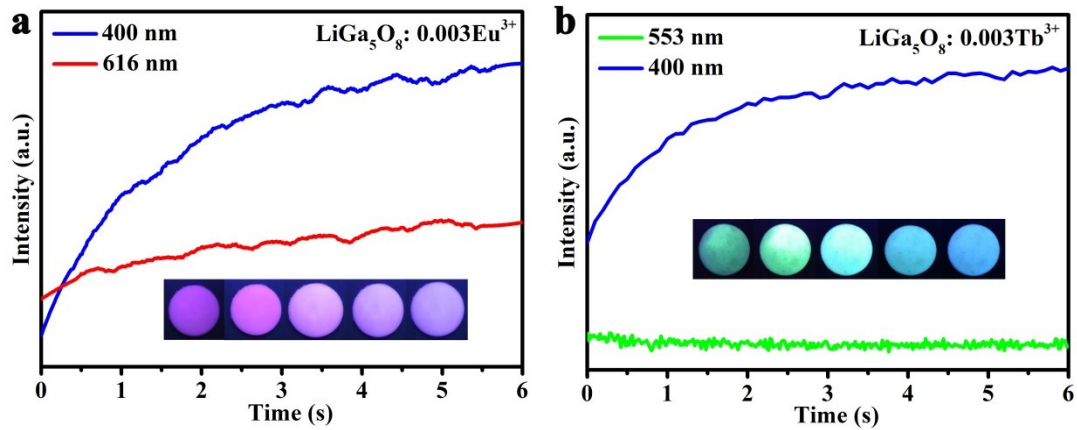


Fig. S5. The emission intensity in the period from 0 s to 6 s.

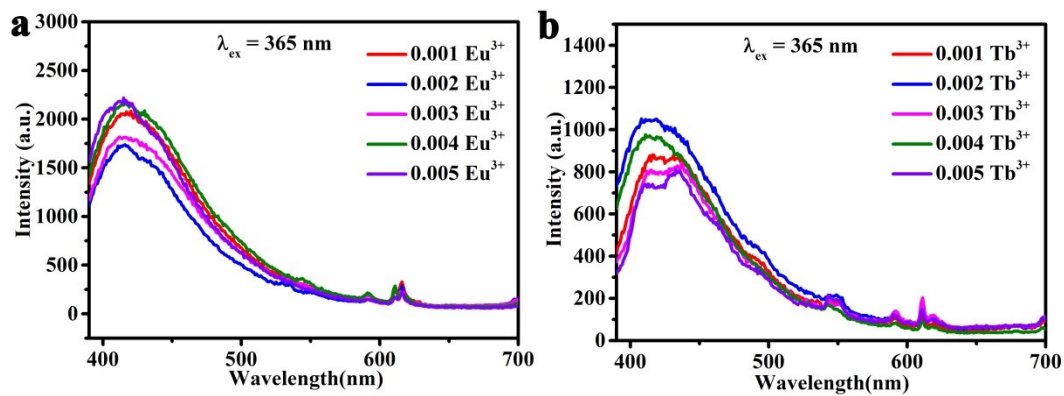


Fig. S6. PL spectra of $\text{LiGa}_5\text{O}_8:\text{xEu}^{3+}$ phosphors and $\text{LiGa}_5\text{O}_8:\text{xTb}^{3+}$ phosphors ($x = 0.001-0.005$).

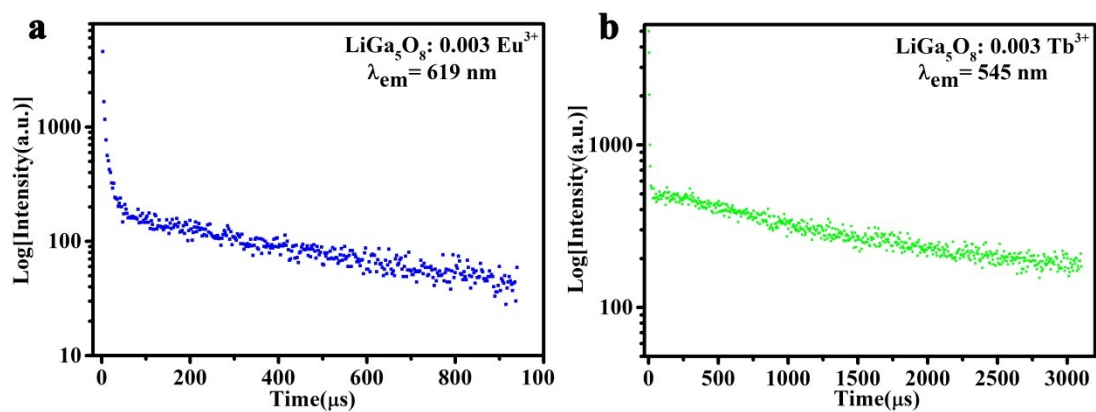


Fig. S7. Fluorescence decay curves of $\text{LiGa}_5\text{O}_8:0.003\text{Eu}^{3+}$ phosphors and $\text{LiGa}_5\text{O}_8:0.003\text{Tb}^{3+}$ phosphors at 254 nm excitation.

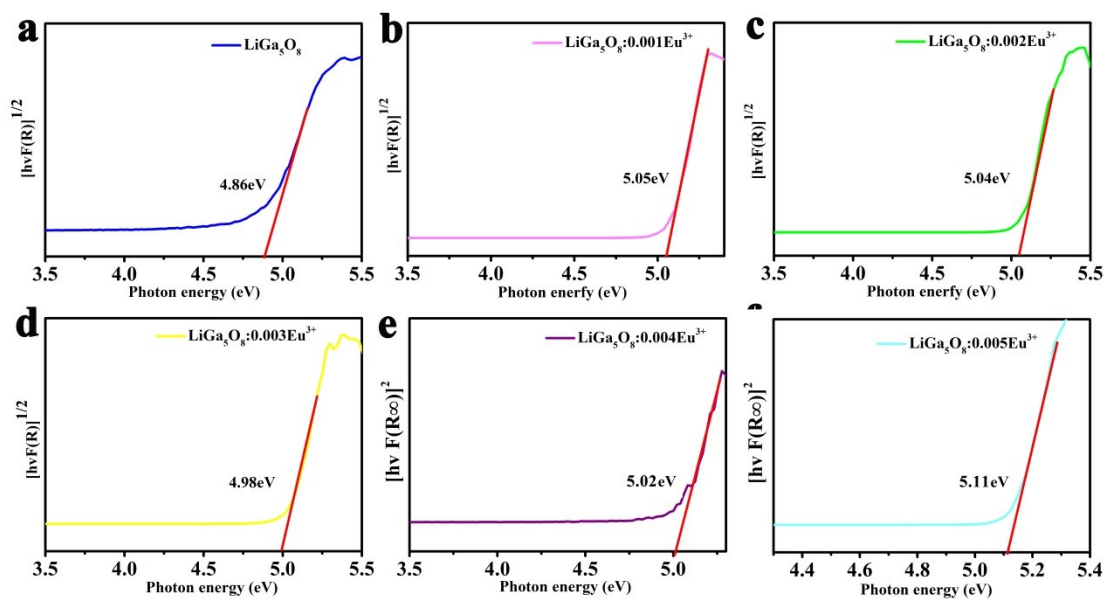


Fig. S8. DR spectra of $\text{LiGa}_5\text{O}_8:\text{xEu}^{3+}$ ($x = 0, 0.001, 0.002, 0.003, 0.004, 0.005$)

phosphors.

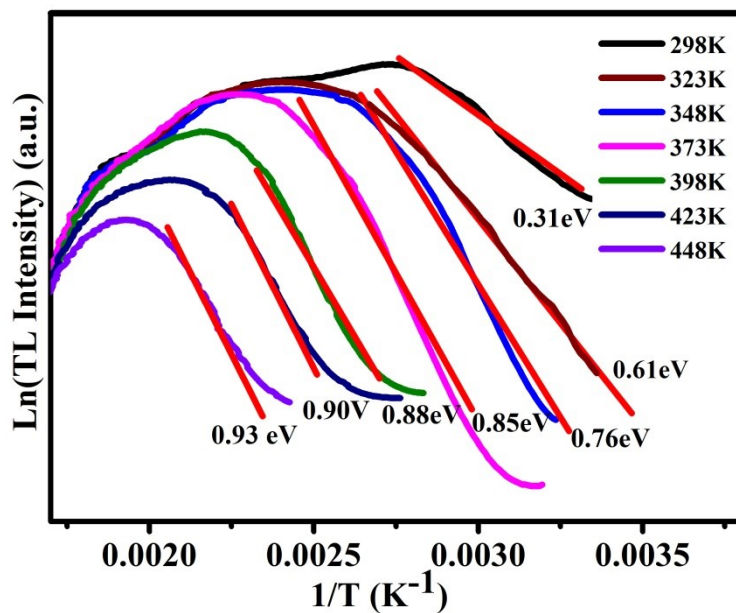


Fig. S9. TL curves analyzed by the initial rising method for trap depth

evaluation.

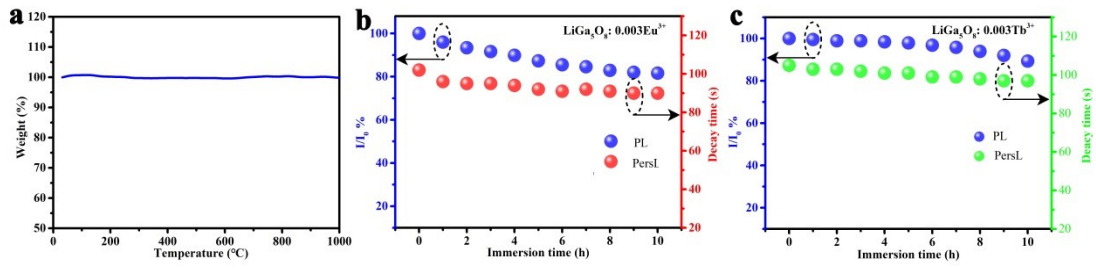


Fig. S10. (a) Thermogravimetric analysis (TGA) data of $\text{LiGa}_5\text{O}_8:0.003\text{Eu}^{3+}$ under inert atmosphere. (b) Water resistance tests of the $\text{LiGa}_5\text{O}_8:\text{Eu}^{3+}$ after being placed in tap water for different time. (c) Water resistance tests of the $\text{LiGa}_5\text{O}_8:\text{Tb}^{3+}$ after being placed in tap water for different time.

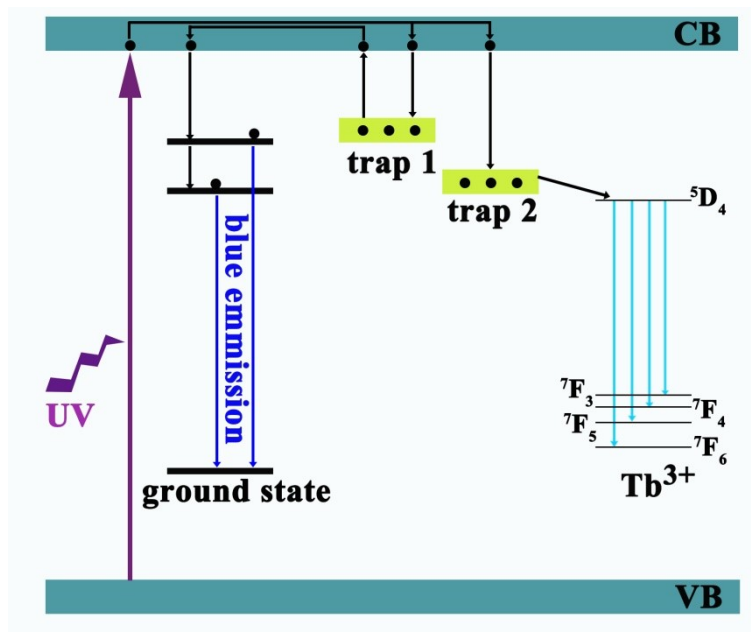


Fig. S11. Energy diagram proposed a plausible afterglow mechanism

Table S1. The refined crystallographic data of LiGa₅O₈.

Formula	LiGa ₅ O ₈
Crystal system	Cubic
Space group	P4332 (212)
Lattice parameters	
a(Å)	8.2130
b(Å)	8.2130
c(Å)	8.2130
$\alpha^\circ=\beta^\circ=\gamma^\circ$	90
Cell volume(Å ³)	553.78
T/K	297
Diffractometer	Rigaku D/Max-2400
Radiation/Å	Cu-Ka ($\lambda= 1.5405$)
Absorption correction	multi-scan
2 θ range $^\circ$ /	10-70
Z	8
Calculated Density	5.3227 g/cm ³
R _{wp}	9.83%
R _p	7.10%

Table S2. Trap parameters and properties based on thermoluminescence peak fitting of LiGa₅O₈:0.003Eu³⁺ phosphors.

Samples	Fitting	E (eV)	b	s (s ⁻¹)	n_0 (cm ⁻³)
LiGa ₅ O ₈ :0.003Eu ³⁺	TL1	0.45	1.13	6.492×10 ⁴	7.713×10 ⁶
	TL2	0.69	1.99	1.044×10 ⁷	6.775×10 ⁶
	TL3	0.72	1.31	2.902×10 ⁶	3.272×10 ⁶
	TL4	0.74	1.35	3.483×10 ⁵	2.848×10 ⁶